2018

A maximum spreading speed for magnetopause reconnection

Geophysical Research Letters

RESEARCH LETTER
10.1029/2018GL078230

Key Points:
- Solar wind fronts can spread across the magnetopause at over 850 km/s
- The speed of solar wind structures contacting the magnetopause does not limit the spreading of magnetic reconnection under typical conditions

Correspondence to:
B. M. Walsh,
bwalsh@bu.edu

Citation:
Walsh, B. M., Welling, D. T., Zou, Y., & Nishimura, Y. (2018). A maximum spreading speed for magnetopause reconnection. *Geophysical Research Letters*, *45*. https://doi.org/10.1029/2018GL078230

Received 8 APR 2018
Accepted 11 MAY 2018
Accepted article online 29 MAY 2018

A Maximum Spreading Speed for Magnetopause Reconnection

B. M. Walsh[1], D. T. Welling[2], Y. Zou[3,4], and Y. Nishimura[3]

[1]Boston University, Center for Space Physics, Department of Mechanical Engineering, Boston, MA, USA, [2]AOSS, University of Michigan, Arbor, MI, USA, [3]Center for Space Physics, Boston University, Boston, MA, USA, [4]Cooperative Programs for the Advancement of Earth System Science, University Corporation for Atmospheric Research, Boulder, CO, USA

Abstract Past observations and numerical modeling find magnetic reconnection to initiate at a localized region and then spread along a current sheet. The rate of spreading has been proposed to be controlled by a number of mechanisms based on the properties within the boundary. At the Earth's magnetopause the spreading speed is also limited by the speed at which a shocked solar wind front can move along the magnetopause boundary. The speed at which a purely north to south rotational discontinuity propagates through the magnetosheath and contacts the magnetopause is measured here using the Block-Adaptive-Tree Solar Wind Roe-Type Upwind Scheme global magnetohydrodynamics model. The propagation speed along the magnetopause is fastest near the nose of the magnetopause and decreases with distance from the subsolar point. The average propagation speed along the dayside magnetopause is 847 km/s. This is significantly larger than observed rates of reconnection spreading at the magnetopause of 30–40 km/s indicating that, for the observed conditions, the speed of front propagation along the magnetopause does not limit or control the spreading rate of reconnection.

Plain Language Summary Energy can transfer from the Sun to the Earth's space environment at varying rates. The results found here dismiss one model that could control the rate of energy change or magnetic reconnection at the edge of the Earth's magnetic field.

1. Introduction

At the start of magnetic reconnection's life cycle is birth and then growth. Birth or initiation is generally thought to occur in a current sheet at a small, localized position and then expand out of the reconnecting plane (Milan et al., 2000; Shay et al., 2003). With application to the Earth's magnetopause, this growth or spreading in the out-of-plane direction occurs across the boundary in local time. Figure 1 presents a diagram of this growth and geometry.

The rate of spreading has significant implications in a number of systems. At a planetary magnetosphere this spreading rate, and subsequently the length of the magnetopause x line, controls how much energy is coupled from the solar wind (Milan et al., 2012). The speed of spreading is relevant for component (Crooker, 1979; Luhmann et al., 1984) and antiparallel (Gonzalez & Mozer, 1974) magnetopause reconnection as well as other local physics-based models predicting the location of reconnection (Hesse et al., 2013; Swisdak & Drake, 2007). This spreading process is also monitored in the solar environment through the elongation of flare ribbons (Li & Zhang, 2009; Qiu et al., 2017; Tripathi et al., 2006), as well as in lab plasmas (Dorfman et al., 2014; Katz et al., 2010).

Several models have been proposed to describe reconnection spreading. At the core of the problem, information needs to be transported away from where reconnection is initiated. One model suggests the expansion is driven by a current out of the reconnecting plane (Huba & Rudakov, 2002; Lapenta et al., 2006; Neeraj et al., 2013; Shay et al., 2003). A second model proposes that reconnection spreading results from Alfvèn waves and would occur at a velocity equal to the out of plane Alfvèn speed (Katz et al., 2010). A third possibility is a combination of the previous two. Here both mechanisms are capable of driving expansion, and the actual speed is the maximum of the two (Shepherd & Cassak, 2012).

These theories and supporting numerical simulations have been based on models with flat current sheets and static boundary conditions. By contrast, a planetary magnetopause is a curved surface and the boundary conditions are temporally variable. A front or discontinuity in the solar wind will pass through the bow shock,

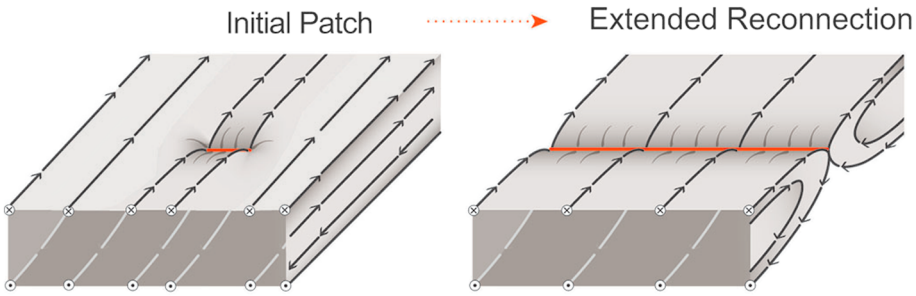

Figure 1. Schematic diagram of reconnection spreading. Initiation occurs in a spatially localized region (left) and spreads into an extended line (right). The region of reconnection is shown in red.

contact the nose of the magnetopause, and then be swept downtail where it contacts the tail magnetopause at later times. If this solar wind discontinuity were a rotation of the magnetic field from purely northward to purely southward, it would strike the subsolar magnetopause first, likely initiating reconnection near local noon, and then contact other places as the front convects tailward in the magnetosheath. The speed of this front's motion through the magnetosheath provides an additional constraint to the spreading speed of magnetopause reconnection. No matter how fast the current carriers or Alfvèn waves may want to propagate, reconnection cannot spread beyond the extent of the high shear angle magnetopause current sheet. The speed of the front along the boundary is therefore the maximum speed of expansion. This paper measures the propagation speed of a rotational discontinuity along the magnetopause in a global magnetohydrodynamic (MHD) model and compares this value with experimentally measured spreading speeds from previous work.

2. Numerical Experiment

The Block-Adaptive-Tree Solar Wind Roe-type Upwind Scheme model (Powell et al., 1999; Tóth et al., 2005, 2012) was run to monitor the propagation of a solar wind front. Grid setup follows that of Welling and Liemohn (2014) with the resolution improved to 1/8 R_E within a block spanning ± 16 R_E in the geocentric solar

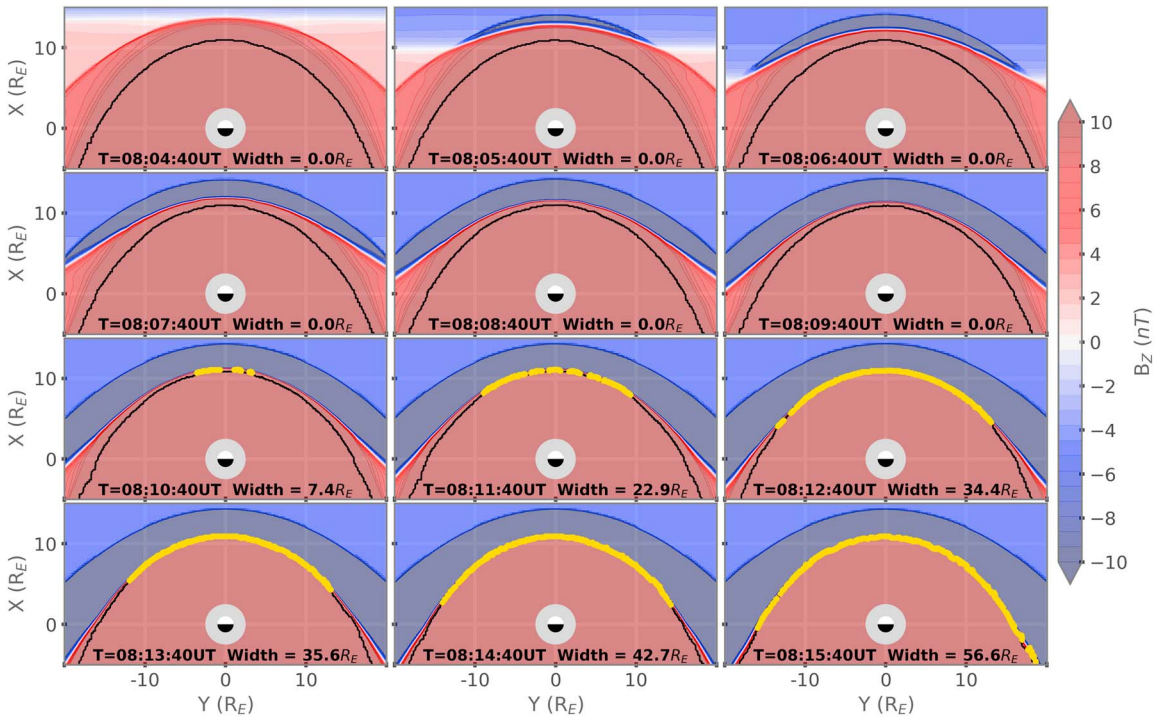

Figure 2. Slices of the *Bz* component of the magnetic field with 1-min time cadence in the *XZ* GSM plane. The yellow dots indicate that a value of −*Bz* is contacting the magnetopause at that local time.

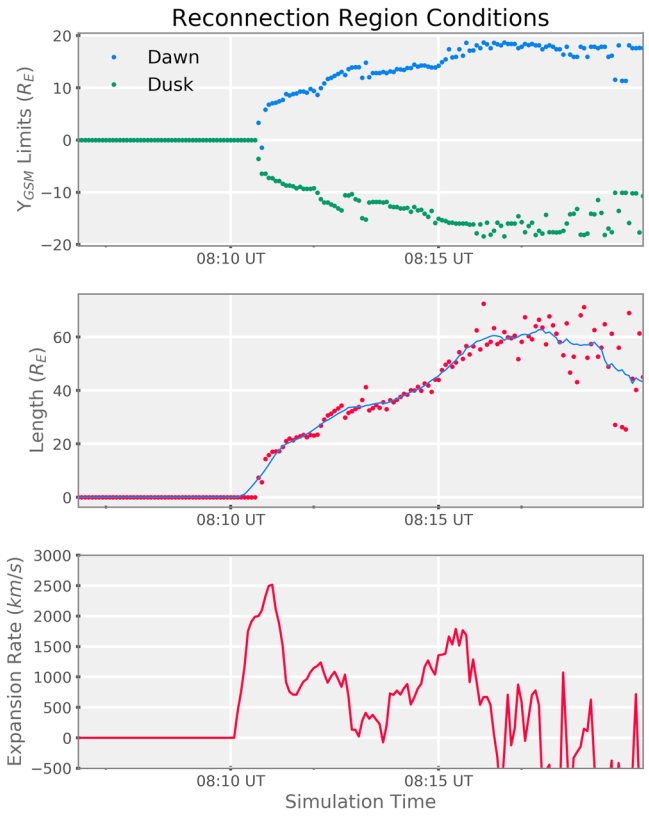

Figure 3. Front spreading along the magnetopause boundary. The top panel presents the GSM *Y* position of the extension of the front in the dawn (blue) and dusk (green) direction. Each point corresponds to a single 5-s MHD step. The middle panel is the length integrated along the magnetopause from the dawn extent to the dusk extent. The blue trace is a running average. The bottom panel is the rate of expansion of the front along the magnetopause. MHD = magnetohydrodynamic.

magnetospheric (GSM) *Y* direction, ± 8 R_E in the GSM *Z* direction, and −4 to +12R_E in the GSM *X* direction. A total of 10.65 million computational cells were used. Solar wind flow conditions were held constant with an earthward flow speed of 400 km/s, a hydrogen number density of 5 cm^{-3}, and a temperature of 1.2×10^5 K. To properly initialize the magnetosphere, the IMF was first southward oriented for 2 hr of simulation time (IMF $B_Z = -2$ nT) and then rotated northward for another 6 hr ($B_Z = +2$ nT), allowing the system to achieve pseudo steady state.

To provide a direct comparison with spreading observations from Zou et al. (2018), the IMF was rotated southward (IMF $B_Z = -5$ nT) at 8 hr into the simulation. As time progressed, the rotational front moved earthward through the magnetosheath and draped along the magnetopause. B_Z contours in the GSM equatorial plane as a function of time are presented in Figure 2. Red contours correspond to regions of northward magnetic field, blue contours show regions of southward magnetic field.

To quantify when and where the front contacted the magnetopause, profiles of *Bz* were drawn radially outward from the Earth. If a $B_Z < 0$ value was measured within 1/4 R_E of the open/closed magnetic field boundary along the radial profile, the front was defined to be "contacting" the magnetopause at that location. Since the resolution of the MHD simulation was 1/8 R_E at the magnetopause, the range spanned two grid points. The boundary between open and closed magnetic field topology was identified through magnetic field line tracing.

The front first contacted the magnetopause near local noon at 8:10:40 in the simulation time. As time continued, the local time of the contacted region along the magnetopause grew. Measurements of the spreading are presented in Figure 3. The top frame shows the limits of the contact region in the GSM *Y* direction; the middle frame shows the integrated length of the contact region along the magnetopause. Although the local time extent of the front's contact region expanded in local time, the rate of expansion was not constant. The bottom panel of Figure 3 presents the expansion rate as a function of time. The largest expansion rate of 2,503 km/s occurred during the 1-min period just as the front contacted the subsolar magnetopause. Although the flow speed in the magnetosheath is low near the subsolar region (Dimmock & Nykyri, 2013; Walsh et al., 2012), there is a relatively large angle between the boundary plane and the Sun-Earth line. This means a small motion of the front in the GSM *X* direction will translate to a large expansion in GSM *Y* and thus local time.

After the brief period (~1 min) with rapid expansion along the boundary, the expansion rate was fairly steady for ~7 min at 825 km/s. During this period the −*Bz* front spread along the boundary to contact a region extending close to 60 R_E in local time. At this point (~8:17 in the simulation) the measured length became variable around a length of 60 R_E and did not expand further. At local times near the terminator the magnetopause boundary became turbulent, and inspection of the bulk flow and magnetic topology presents evidence for boundary waves and flux transfer events. Additionally, the magnetopause boundary increased in thickness with distance from local noon. As the boundary becomes thicker it will not be detected as a "contacted" boundary with the used metric. These conditions may limit the ability to measure expansion beyond the terminator; however, since the primary objective in the study is to measure expansion speeds along the dayside magnetopause, they are not problematic.

3. Discussion

As the front moved through the bow shock and into the magnetosheath it bent around the obstacle of the magnetosphere. Similar results have been found experimentally through studies monitoring how an interplanetary shock passed through the magnetosheath (Keika et al., 2009). Although many fronts that contact the magnetopause are close to perpendicular to the Earth-Sun line, they can also be inclined or have

Table 1
Spreading Speeds at the Magnetopause

Type		Value
Theory-Alfvèn speed	v_{Alfven} [a]	71.6 km/s
Theory-Current speed	v_J [a]	89.8 km/s
Experimental ionosphere	$v_{Observed}$ [a]	39.9 km/s
Numerical front speed	$v_{MHD\ Front}$	847 km/s

[a]Values from Zou et al. (2018).

different orientations. Studies modeling the dynamics of inclined shocks striking the magnetopause have shown as a structure becomes more inclined, the position at which it first strikes the magnetopause moves away from the subsolar point (Oliveira & Raeder, 2014; Samsonov, 2011; Samsonov et al., 2015). The geometry where a front first strikes the magnetopause will in turn impact the spreading speed. Since the ionospheric signatures of reconnection in the event being simulated here commence near local noon, it is reasonable to assume the front was close to perpendicular to the Earth-Sun line.

3.1. Front Propagation Speeds and Reconnection Spreading

At a planetary magnetosphere embedded within a flowing solar wind, IMF structures will strike the nose of the magnetopause and then propagate tailward along the boundary. This speed of propagation will limit the maximum spreading speed of magnetic reconnection in the system. In the case of a discontinuity in the solar wind with a rotation from positive to negative *Bz*, reconnection is anticipated to be initialized at the subsolar point of the magnetopause when the discontinuity contacts the boundary. No matter how quickly reconnection may want to spread, the process is limited by the propagation speed of the magnetosheath magnetic field discontinuity along the magnetopause. For some boundary conditions, this process may not limit reconnection spreading. In a current sheet with very little guide field and a small current, one may not anticipate reconnection to spread quickly based on current theory. By contrast, for a boundary with a large guide field (large out of plane Alfvèn speed) or a large current velocity, reconnection may be limited by the magnetosheath front speed.

3.2. Comparison With Past Measurements

Using projected measurements of ionospheric flows, Zou et al. (2018) were able to create estimates for magnetopause reconnection spreading rates. In the two events analyzed, the measured spreading rates were less than those predicted by theory. Table 1 presents the spreading speeds obtained by Zou et al. (2018) from 23 May 2014 as well as the front velocity from the current study. As noted previously, theory predicts that the spreading speed will be the maximum velocity of either the out of plane Alfvèn speed (v_A) or the current carrier speed (v_J; Shepherd & Cassak, 2012). The out of plane Alfvèn speed is described as $v_A = \frac{B_m}{\sqrt{\mu_0 \rho}}$ where B_m is the out of plane magnetic field or guide field, μ_0 is the permeability of free space, and ρ is the mass density. The current velocity is $v_J = \frac{J}{ne}$ where J is the current density, n is the number density, and e is the charge of an electron. The upstream solar wind conditions in the current study were chosen to match those from the 23 May 2014 event. The expansion speed of the front along the boundary found through MHD is more than an order of magnitude larger than the measured and theoretical values of the reconnection spreading speed. This indicates that the front expansion speed does not play a significant role in controlling or limiting the spreading speed.

3.3. Reconnection Rotation

A possible alternative model to spreading reconnection is that reconnection is always active somewhere at the magnetopause. In this model, rather than starting as a small patch and growing, an extended x line is omnipresent and will just shift its position in response to IMF rotations or changes in the solar wind. Although the community has long studied the steady state location of dayside magnetopause reconnection (Pu et al., 2007; Trenchi et al., 2008), very little observational work has been conducted monitoring the dynamic motion (or death) of an x line. One requirement of the "rotating reconnection line" model is that structures or regions of active reconnection along the magnetopause boundary can be relatively steady and will sometimes move sunward during rotations. Hybrid and kinetic numerical modeling results are not consistent with this picture. These models present a dynamic system where reconnection commonly turns on, off, and moves tailward, even for steady solar wind conditions (Hoilijoki et al., 2017; Sibeck & Omidi, 2012). In these models it is uncommon for reconnecting structures to move in the sunward direction.

Observations have also reported magnetopause reconnection to be both limited (Milan et al., 2016; Oksavik et al., 2004; Walsh et al., 2017) as well as extended in local time (Dunlop et al., 2011; Phan et al., 2000). Varying spatial extents along the boundary is consistent with a model where reconnection can be transient and growing with time. It is not strictly consistent with an omnipresent reconnection line. Similar results are found in the ionosphere. Rather than an omnipresent aurora or region of convection that may result from omnipresent magnetopause reconnection, ionospheric measurements find signatures that fade/die

and reform corresponding to different regions of reconnection turning off and on at the magnetopause (Sandholt & Farrugia, 2002; Zou et al., 2018).

3.4. Observational Signatures

If the rotational front indeed passes by the magnetosphere faster than reconnection can spread in local time from the point of first contact, there are several features that should be observable with spacecraft measurements. Depending on how reconnection manifests, an observer should either find discontinuous patches of reconnection or time periods where reconnection is observed near local noon but not at other local times. The patchy reconnection scenario would occur once a front of $-Bz$ in the magnetosheath has draped itself over a range of local times at the magnetopause, but the initial patch of reconnection near local noon has not had time to spread. This would leave large spatial areas with significant magnetic shear at the magnetopause that could reconnect locally and start spreading themselves. This is similar to the scenario found in simulations of the magnetotail plasma sheet where many spatially localized patches form initially and coalesce into a larger continuous x line (Shay et al., 2003).

Alternatively, a scenario may exist where reconnection can only be initiated at the nose of the magnetopause or the place of first contact. This may be due to the thickness of the boundary layer or the presence of stabilizing flows in the magnetosheath off local noon. In this scenario, once again, one should be able to observe active reconnection at or near local noon but regions away from noon with large magnetic sheath and no active reconnection.

4. Conclusions

A global Block-Adaptive-Tree Solar Wind Roe-Type Upwind Scheme MHD simulation was used to monitor the rate at which a $+Bz$ to $-Bz$ discontinuity passed through the magnetosheath and draped along the magnetopause. The expansion speed of a front along the magnetopause boundary is important as it serves as a limit for the maximum spreading speed of magnetopause reconnection. The $-Bz$ front contacted the nose of the magnetopause and expanded past the terminator in 7 min, corresponding to an average expansion speed in local time along the boundary of 847 km/s. The simulation was designed with similar solar wind conditions to a previous observational experiment that found magnetopause reconnection to expand at 30–40 km/s. Since the front expansion is much larger than the observed spreading rates it is concluded that the expansion rate of a solar wind front along the magnetopause does not limit the spreading rate for the current event and others with similar solar wind conditions.

Acknowledgments

Support was given by the NASA grants NNX16AJ73G and NNX16AD91G. NSF support was provided by grant AGS-1502436. Analysis of the MHD results was performed using the Spacepy software library (Morley et al., 2011). The authors would like to thank R. Lopez for useful discussions. MHD simulation files generated and used as part of this study are available online through the following: https://deepblue.lib.umich.edu/data/concern/genericworks/sj1392745?locale=en.

References

Crooker, N. U. (1979). Dayside merging and cusp geometry. *Journal of Geophysical Research*, *84*(A3), 951–959. https://doi.org/10.1029/JA084iA03p00951

Dimmock, A. P., & Nykyri, K. (2013). The statistical mapping of magnetosheath plasma properties based on THEMIS measurements in the magnetosheath interplanetary medium reference frame. *Journal of Geophysical Research: Space Physics*, *118*, 4963–4976. https://doi.org/10.1002/jgra.50465

Dorfman, S., Ji, H., Yamada, M., Yoo, J., Lawrence, E., Myers, C., & Tharp, T. (2014). Experimental observation of 3-D, impulsive reconnection events in a laboratory plasma. *Physics of Plasmas*, *21*(1), 012109. https://doi.org/10.1063/1.4862039

Dunlop, M. W., Zhang, Q. -H., Bogdanova, Y. V., Trattner, K. J., Pu, Z., Hasegawa, H., et al. (2011). Magnetopause reconnection across wide local time. *Annales Geophysicae*, *29*, 1683–1697. https://doi.org/10.5194/angeo-29-1683-2011

Gonzalez, W. D., & Mozer, F. S. (1974). A quantitative model for the potential resulting from reconnection with an arbitrary interplanetary magnetic field. *Journal of Geophysical Research*, *79*(28), 4186–4194. https://doi.org/10.1029/JA079i028p04186

Hesse, M., Aunai, N., Zenitani, S., Kuznetsova, M., & Birn, J. (2013). Aspects of collisionless magnetic reconnection in asymmetric systems. *Physics of Plasmas*, *061210*(6). https://doi.org/10.1063/1.4811467

Hoilijoki, S., Ganse, U., Pfau-Kempf, Y., Cassak, P. A., Walsh, B. M., Hietala, H., et al. (2017). Reconnection rates and X line motion at the magnetopause: Global 2D-3V hybrid-Vlasov simulation results. *Journal of Geophysical Research: Space Physics*, *122*, 2877–2888. https://doi.org/10.1002/2016JA023709

Huba, J. D., & Rudakov, L. I. (2002). Three-dimensional Hall magnetic reconnection. *Physics of Plasmas*, *9*, 4435.

Katz, N., Egedal, J., Fox, W., Le, A., Bonde, J., & Vrublevskis, A. (2010). Laboratory observation of localized onset of magnetic reconnection. *Physical Review Letters*, *104*(25), 255004. https://doi.org/10.1103/PhysRevLett.104. 255004

Keika, K., Nakamura, R., Baumjohann, W., Angelopoulos, V., Kabin, K, Glassmeier, K. H., et al. (2009). Deformation and evolution of solar wind discontinuities through their interactions with the Earth's bow shock. *Journal of Geophysical Research*, *114*, A00C26. https://doi.org/10.1029/2008JA013481

Lapenta, G., Krauss-Varban, D., Karimabadi, H., Huba, J. D., Rudakov, L. I., & Ricci, P. (2006). Kinetic simulations of X-line expansion in 3D reconnection. *Geophysical Research Letters*, *33*, L10102. https://doi.org/10.1029/2005GL025124

Li, L., & Zhang, J. (2009). On the brightening propagation of post-flare loops observed by TRACE. *Astrophysical Journal*, *690*, 13. https:/doi.org/10.1088/0004-637X/690/1/347

Luhmann, J. G., Walker, R. J., Russell, C. T., Crooker, N. U., Spreiter, J. R., & Stahara, S. S. (1984). Patterns of potential magnetic field merging sites on the dayside magnetopause. *Journal of Geophysical Research*, *89*(A3), 1739–1742. https://doi.org/10.1029/JA089iA03p01739

Milan, S. E., Gosling, J. S., & Hubert, B. (2012). Relationship between interplanetary parameters and the magnetopause reconnection rate quantified from observations of the expanding polar cap. *Journal of Geophysical Research*, *117*, A03226. https://doi.org/10.1029/2011JA017082

Milan, S. E., Imber, S. M., Carter, J. A., Walach, M.-T., & Hubert, B. (2016). What controls the local time extent of flux transfer events. *Journal of Geophysical Research: Space Physics*, *121*, 1391–1401. https://doi.org/10.1002/2015JA022012

Milan, S. E., Lester, M., Cowley, S. W. H., & Brittnacher, M. (2000). Convection and auroral response to a southward turning of the IMF: Polar UVI, CUTLASS, and IMAGE signatures of transient magnetic flux transfer at the magnetopause. *Journal of Geophysical Research*, *105*(A7). https://doi.org/10.1029/2000JA900022

Morley, S., Welling, D., Koller, J., Larsen, B. A., Henderson, M. G., & Niehof, J. (2011). SpacePy—A python-based library of tools for the space sciences. In *Proceeding of the 9th Python in Science Conference* (pp. 39–45). Austin, TX.

Neeraj, J., Buchner, J., Dorfman, S., Ji, H., & Sharma, A. S. (2013). Current disruption and its spreading in collisionless magnetic reconnection. *Physics of Plasmas*, *20*(11), 112101. https://doi.org/10.1063/1.4827828

Oksavik, K., Moen, J., & Carlson H. C. (2004). High-resolution observations of the small-scale flow pattern associated with a poleward moving auroral form in the cusp. *Geophysical Research Letters*, *31*, L11807. https://doi.org/10.1029/2004GL019838

Oliveira, D. M., & Raeder, J. (2014). Impact angle control of interplanetary shock geoeffectiveness. *Journal of Geophysical Research: Space Physics*, *119*, 8188–8201. https://doi.org/10.1002/2014JA020275

Phan, T. D., Kistler, L., Klecker, B., Haerendel, G., Paschmann, G., Sonnerup, B. U. Ö., et al. (2000). Extended magnetic reconnection at the Earth's magnetopause from detection of bi-directional jets. *Nature*, *404*(6780), 848–850. https://doi.org/10.1038/35009050

Powell, K. G., Roe, P. L., Linde, T. J., Gombosi, T. I., & De Zeeuw, D. L. (1999). A solution-adaptive upwind scheme for ideal magnetohydrodynamics. *Journal of Computational Physics*, *154*(2), 284–309.

Pu, Z. Y., Zhang, X. G., Wang, X. G., Wang, J., Zhou, X.-Z., Dunlop, M. W., et al. (2007). Global view of dayside magnetic reconnection with the dusk-dawn IMF orientation: A statistical study for Double Star and Cluster data. *Geophysical Research Letters*, *34*, L20101. https://doi.org/10.1029/2007GL030336

Qiu, J., Longcope, D. W., Cassak, P. A., & Priest, E. R. (2017). Elongation of flare ribbons. *Astrophysical Journal*, *838*(17), 838–855. https://doi.org/10.3847/1538-4357/aa6341

Samsonov, A. A. (2011). Propagation of inclined interplanetary shock through the magnetosheath. *Journal of Atmospheric and Solar-Terrestrial Physics*, *73*, 30–39. https://doi.org/10.1016/j.jastp.2009.10.014

Samsonov, A. A., Sergeev, V. A., Kuznetsova, M. M., & Sibeck, D. G. (2015). Asymmetric magnetospheric compressions and expansions in response to impact of inclined interplanetary shock. *Geophysical Research Letters*, *42*, 4716–4722. https://doi.org/10.1002/2015GL064294

Sandholt, P. E., & Farrugia, C. J. (2002). Monitoring magnetosheath? magnetosphere interconnection topography from the aurora. *Annales Geophysicae*, *20*, 629.

Shay, M. A., Drake, J. F., Swisdak, M., Dorland, W., & Rogers, B. N. (2003). Inherently three-dimensional magnetic reconnection: A mechanism for bursty bulk flows? *Geophysical Research Letters*, *30*(6), 1345. https://doi.org/10.1029/2002GL016267

Shepherd, L. S., & Cassak, P. A. (2012). Guide field dependence of 3-D X-line spreading during collisionless magnetic reconnection. *Journal of Geophysical Research*, *117*, A10101. https://doi.org/10.1029/2012JA017867

Sibeck, D. G., & Omidi, N. (2012). Flux transfer events: Motion and signatures. *Journal of Atmospheric and Solar-Terrestrial Physics*, *87*, 20–24. https://doi.org/10.1016/j.jastp.2011.07.010

Swisdak, M., & Drake, J. F. (2007). Orientation of the reconnection X-line. *Geophysical Research Letters*, *34*, L11106. https://doi.org/10.1029/2007GL029815

Tóth, G., Sokolov, I. V., Gombosi, T. I., Chesney, D. R., Clauer, C. R., De Zeeuw, D. L., et al. (2005). Space weather modeling framework: A new tool for the space science community. *Journal of Geophysical Research*, *110*, A12226. https://doi.org/10.1029/2005JA011126

Tóth, G., van der Holst, B., Sokolov, I. V., De Zeeuw, D. L., Gombosi, T. I., Fang, F., et al. (2012). Adaptive numerical algorithms in space weather modeling. *Journal of Computational Physics*, *231*, 870–903.

Trenchi, L., Marcucci, M. F., Pallocchia, G., Consolini, G., Bavassano Cattaneo, M. B., Di Lellis, A. M., et al. (2008). Occurrence of reconnection jets at the dayside magnetopause: Double Star observations. *Journal of Geophysical Research*, *113*, A07S10. https://doi.org/10.1029/2007JA012774

Tripathi, D., Isobe, H., & Mason, H. E. (2006). On the propagation of brightening after filament/prominence eruptions, as seen by SoHO-EIT. *Astronomy and Astrophysics*, *453*, 1111–1116. https://doi.org/10.1051/0004-6361:20064993

Walsh, B. M., Komar, C. M., & Pfau-Kempf, Y. (2017). Spacecraft measurements constraining the spatial extent of a magnetopause reconnection X line. *Geophysical Research Letters*, *44*, 3038–3046. https://doi.org/10.1002/2017GL073379

Walsh, B. M., Sibeck, D. G., Wang, Y., & Fairfield, D. H. (2012). Dawn-dusk asymmetries in the Earth's magnetosheath. *Journal of Geophysical Research*, *117*, A12211. https://doi.org/10.1029/2012JA018240

Welling, D. T., & Liemohn, M. W. (2014). Outflow in global magnetohydrodynamics as a function of a passive inner boundary source. *Journal of Geophysical Research: Space Physics*, *119*, 2691–2705. https://doi.org/10.1002/2013JA019374

Zou, Y., Walsh, B. M., Nishimura, Y., Angelopoulos, V., Ruohoniemi, J. M., McWilliams, K. A., & Nishitani, N. (2018). Spreading speed of magnetopause reconnection X-lines using ground-satellite coordination. *Geophysical Research Letters*, *45*, 80–89. https://doi.org/10.1002/2017GL075765